Effect of geometric anisotropy on optical nonlinearity enhancement for periodic composites

Baifeng Yang,[1] Chengxiang Zhang,[2] and Decheng Tian[1]
[1]*Department of Physics, Wuhan University, Wuhan 430072, People's Republic of China*
[2]*Department of Physics, Jilin University, Changchun 130023, People's Republic of China*
(Received 5 September 2002; published 22 January 2003)

The effect of geometric anisotropy on the optical nonlinearity enhancement for the composites with metal or semiconductor spheriodal-shaped particles periodically in an insulating host is investigated. The frequency dependences of effective nonlinear susceptibility are calculated with the Stroud-Hui relation and a series expression of space-dependent electric field in periodic composites. The results show that for both metal-insulator (MI) and semiconductor-insulator (SI) composites, nonlinearity enhancement increases almost to its maximum when the percolation networks of the inclusion phase form. The nonlinearity enhancement increases to its maximum when the composites are transformed into the Boyd-Sipe layered composites. The behavior of the nonlinearity enhancement near the percolation threshold is also investigated. A local minimum appears in the nonlinear optical responses at the percolation threshold for the MI composites. For the SI composites the local minimum appears when the ratio of the bound-electron number density to the effective mass of the electron is large.

DOI: 10.1103/PhysRevB.67.045106 PACS number(s): 78.20.−e, 42.65.An, 81.40.Tv

I. INTRODUCTION

Nonlinear-optical materials are of great practical importance for future applications in real-time holography, optical correlators, phase-conjugators, and thresholding device.[1,2] The optical nonlinearity enhancement of granular composite materials has been extensively studied in recent years.[2–12] The composites of interest are usually made of nonlinear metal or semiconductor particles embedded in an insulating host. Nonlinear susceptibility of the composites can be strongly enhanced relative to those of component materials. Anisotropy of microstructure of composite materials has a pronounced effect on the nonlinearity enhancement. Within effective-medium approximation (EMA), Yuen *et al.* investigated the optical nonlinearity enhancement of metal granular composites with electric-field induced anisotropic microstructure.[3] Haus *et al.* studied the nonlinearity enhancement by using ellipsoidal (specifically, spheroidal-shaped) particles.[4] In this work, we study the anisotropic composites, anisotropy of which stems from the geometric morphology of inclusions.

The anisotropic composites studied here are composed of identical spheroidal-shaped particles made of an isotropic metal or semiconductor, embedded in an isotropic linear insulating host in a simple cubic lattice. The orientations of the principal axes of the spheroids are to be coincident with the lattice axes. The effective third-order optical nonlinearity of the composites is now a function of the aspect ratio $\eta = c/a$, where a and c are the lengths of semiaxes of the spheroids in the $x(y)$ and the z directions, respectively. Our studies mainly concern the composites consisting of oblate spheroids, that is, $\eta \leqslant 1$ $(c \leqslant a)$. An electric field is applied along the minor axis, i.e., along the c axis. By changing the aspect ratio of the spheroids and keeping the volume fraction of the inclusions unchanged, various kinds of microstructure of the composites are formed. At first, each particle is within a unit cell [see Fig. 1(a)]. We call this kind of structure nonoverlapping. With a decrease in η, the particles will approach their neighborhoods in the same x,y-plane. When the aspect ratio reaches a critical value, the particles in each x,y-plane will touch one another, and series of two-dimensional percolation networks are formed. As the aspect ratio decreases further, the neighboring particles in the same x,y-plane will overlap, and the inclusion phase forms layers with holes periodically arranged in them [see Fig. 1(b)], and furthermore, the composite forms a structure with layers of fluctuating thickness. We call these kinds of structure overlapping. The extreme case of overlapping is a layered structure with flat interfaces.

With the Stroud-Hui expression for the effective third-order optical nonlinearity χ_e,[5] and an exact series expression of the local electric field in periodic composites,[6] the χ_e of the composites is calculated for various kinds of microstructure. The results show that the third-order optical nonlinearity reaches almost to its maximum when the percolation networks of the inclusion phase form. The χ_e has little increase when the fluctuation of the thickness of the layers decreases further.

A theory developed recently predicted that at percolation there is a minimum in nonlinear optical responses in metal-insulator (MI) composites.[7] Analogous conclusion is obtained in our calculations, although the percolation networks in Ref. 7 and in this work are formed by different mechanisms. In Ref. 7 it is formed by increasing the volume fraction of inclusions, here it is formed by changing the shape of the inclusions and keeping the volume fraction of the inclusions constant.

II. THEORY

For a composite with weakly nonlinear components, to first order in the nonlinear susceptibility of the components, the effective third-order nonlinear susceptibility is given as[8]

$$\chi_e = \sum_i p_i \chi_i \langle |\mathbf{E}_{lin}(\mathbf{r})|^2 \mathbf{E}_{lin}^2(\mathbf{r}) \rangle_i / \mathbf{E}_0^4, \qquad (1)$$

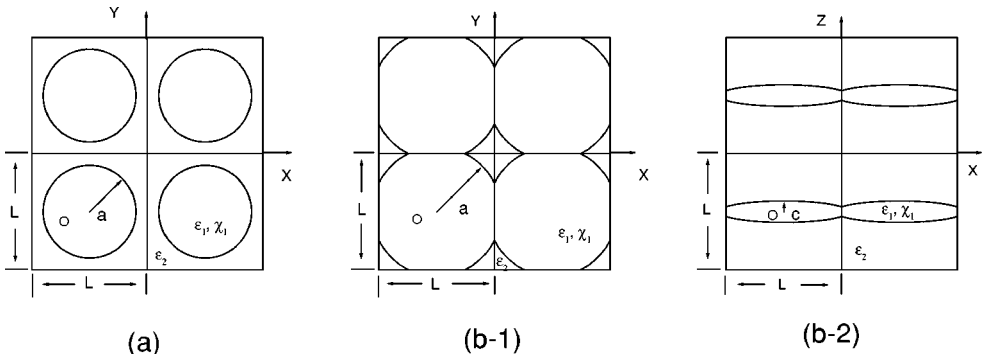

FIG. 1. Schematic drawing of four unit cells for $\eta<1$; (a) nonoverlapping oblate spheroids with semiaxes a and c, all are less than $L/2$, (b) layered networks with holes composed of the truncated oblate spheroids with semi-axes a and c. Here a is larger than $L/2$ but less than $L/\sqrt{2}$ and c is less than $L/2$.

where χ_i and p_i are the third-order nonlinear susceptibility and the volume fraction of the ith component, respectively. $\langle\,\rangle_i$ denotes a volume average over the volume of the ith component, $\mathbf{E}_0$ is the applied electric field and $\mathbf{E}_{lin}$ is the electric field in the linear limit where $\chi_i=0$.

For the geometric morphology considered here, the effective third-order nonlinear susceptibility of the composites is a diagonal tensor and its components $\chi_e^{\alpha\alpha}$ $(\alpha=x,y,z)$ can be expressed as

$$\chi_e^{\alpha\alpha}=\frac{\chi_1}{V}\int_{V_1}|\mathbf{E}_{lin}(\mathbf{r})|^2\mathbf{E}_{lin}^2(\mathbf{r})d\mathbf{r}/\mathbf{E}_0^4, \tag{2}$$

where V is the volume of a unit cell and V_1 is the volume of the nonlinear phase (inclusion phase) in the unit cell. The enhancement factor in the α direction $g_e^{\alpha\alpha}$ is defined as

$$g_e^{\alpha\alpha}=\chi_e^{\alpha\alpha}/\chi_1. \tag{3}$$

We assume that the size of the particles is much smaller than the optical wavelength, therefore the quasistatic approximation can be used. The space-dependent electric field $\mathbf{E}_{lin}(\mathbf{r})$ in the linear case for a two-component periodic composite is expressed as the series[6]

$$\mathbf{E}_{lin}(\mathbf{r})=E_0\left\{\hat{\mathbf{e}}+\sum_{l=1}^{\infty}(1/w)^l\mathbf{C}_l^E(\mathbf{r})\right\}, \tag{4}$$

where

$$w=\frac{p_1\varepsilon_1+p_2\varepsilon_2}{\varepsilon_2-\varepsilon_1}, \tag{5}$$

$$\mathbf{C}_l^E(\mathbf{r})=\sum_{\mathbf{k}_1}{}'\cdots\sum_{\mathbf{k}_l}{}'\hat{\mathbf{k}}_1\exp(i\mathbf{k}_1\cdot\mathbf{r})(\hat{\mathbf{k}}_1\cdot\hat{\mathbf{k}}_2)\theta_1(\mathbf{k}_1-\mathbf{k}_2)\cdots(\hat{\mathbf{k}}_{l-1}\cdot\hat{\mathbf{k}}_l)\theta_1(\mathbf{k}_{l-1}-\mathbf{k}_l)(\hat{\mathbf{k}}_l\cdot\hat{\mathbf{e}})\theta_1(\mathbf{k}_l). \tag{6}$$

In the above relations, $\hat{\mathbf{e}}$ is a unit vector in the direction of $\mathbf{E}_0$, $\mathbf{k}$ is the reciprocal vector of the periodic structure, $\hat{\mathbf{k}}$ is the unit vector in the $\mathbf{k}$ direction, $\Sigma'_{\mathbf{k}_i}$ indicates that the summation is over $\mathbf{k}_i$ for $\mathbf{k}_i\neq0$ and $\mathbf{k}_i\neq\mathbf{k}_{i-1}$, and

$$\theta_1(\mathbf{k})=\frac{1}{V}\int_{V_1}\exp(-i\mathbf{k}\cdot\mathbf{r})d\mathbf{r} \tag{7}$$

is the Fourier coefficient of the indicator function of the first component,[14] which depends on the shape of the inclusions.

The spheroids can be characterized by the aspect ratio $\eta=c/a$. Here we only consider this kind of geometric structures that the inclusion particles are oblate spheroids, therefore we always have $\eta\leqslant1$ $(c\leqslant a)$. $\eta=1$ corresponds to the structure where the inclusions are spheres. For a composite with a fixed value of the volume fraction of inclusions, there are two special values of η, denoted $\eta_c^{(1)}$ and $\eta_c^{(2)}$,

$$\eta_c^{(1)}=\frac{6p'}{\pi},\quad \eta_c^{(2)}=\frac{3p'}{\sqrt{2}\pi},\quad p'=\frac{4\pi a^2c}{3V}. \tag{8}$$

When $\eta>\eta_c^{(1)}$, $a<L/2$, where L is the lattice constant, and the composite consists of isolated (nonoverlapping) spheroidal inclusions. $\eta=\eta_c^{(1)}$ corresponds to the case where $a=L/2$ and the neighboring spheroids in each x-y plane just touch one another. For these two kinds of microstructure,

$$\theta_1^{(\mathrm{noe})}(\mathbf{k})=3p_1[\sin(\overline{ka})-(\overline{ka})\cos(\overline{ka})]/(\overline{ka})^3, \tag{9}$$

where p_1 is the volume fraction of inclusions,

$$p_1=\frac{V_1}{V}=\frac{4\pi\eta}{3}\left(\frac{a}{L}\right)^3, \tag{10}$$

and $\overline{k}$ satisfies

$$\overline{k^2}=k_x^2+k_y^2+(\eta k_z)^2; \tag{11}$$

here $(k_x,k_y,k_z)=(2\pi/L)(n_x,n_y,n_z)$ and n_x,n_y,n_z are integers.

When $\eta_c^{(2)}<\eta<\eta_c^{(1)}$, $L/2<a<L/\sqrt{2}$, and the neighboring spheroids in the same x-y plane will overlap, the inclusion phase forms layers with holes periodically arranged in them. The real shape of the inclusions is not a spheroid, but only the part of the spheroids within the unit cell. In this case, we can evaluate the Fourier coefficient $\theta_1(\mathbf{k})$ by dividing the volume integral in Eq. (7) into several parts. With a

procedure analogous to that used in Ref. 15, Fourier coefficients of the indicator function of the inclusion phase can be expressed as

$$\theta_1^{(\mathrm{oe})}(\mathbf{k})=\theta_1^{(\mathrm{noe})}(\mathbf{k})-[F(\bar{k}_{xz},k_y)+F(\bar{k}_{yz},k_x)]=I(\bar{k}_{xz},k_y)+I(\bar{k}_{yz},k_x)-\theta_1^{(\mathrm{noe})}(\mathbf{k}). \tag{12}$$

In this relation,

$$F(\bar{k}_{yz},k_x)=\frac{4\pi\eta}{L^3\bar{k}_{yz}}\int_{L/2}^{a}\sqrt{a^2-x^2}\cos(k_x x)J_1(\bar{k}_{yz}\sqrt{a^2-x^2})dx, \tag{13}$$

$$I(\bar{k}_{yz},k_x)=\frac{4\pi\eta}{L^3\bar{k}_{yz}}\int_{0}^{L/2}\sqrt{a^2-x^2}\cos(k_x x)J_1(\bar{k}_{yz}\sqrt{a^2-x^2})dx, \tag{14}$$

where $\bar{k}_{yz}$ satisfies

$$\bar{k}_{yz}^2=k_y^2+(\eta k_z)^2, \tag{15}$$

and $J_1(x)$ represents the Bessel function. In the calculation of Eq. (12), the integrand in Eq. (14) can be expanded as a double series form (cf. Ref. 15)

$$I(\bar{k}_{yz},k_x)=\frac{2\pi\eta}{L^3}\sum_{n=0}^{\infty}\frac{1}{n!}\left(-\frac{\bar{k}_{yz}^2a^2}{4}\right)^n\times\sum_{l=0}^{n+1}\frac{(-1)^l a^{-2l+2}}{l!(n+1-l)!}\int_0^{L/2}x^{2l}\cos(k_x x)dx. \tag{16}$$

That is, n in the denominator should be corrected as $n!$ ($n!$ denotes the factorial of n); l in the denominator should be corrected as $l!$ ($l!$ denotes the factorial of l); $(k+1-l)$ in the denominator should be corrected as $(n+1-l)!$ and please take note of the position of superscript n.

In the case of $k_x=0$,

$$I(\bar{k}_{yz},0)=-2\pi\eta\frac{a}{\bar{k}_{yz}L^2}\sum_{l=0}^{\infty}\frac{J_{l-1}(\bar{k}_{yz}a)}{l!(2l+1)}\left(\xi\frac{\bar{k}_{yz}a}{2}\right)^l, \tag{17}$$

where $\xi=L/(2a)$. In the general case of $k_x\neq 0$,

$$I(\bar{k}_{yz},k_x)=(-1)^{n_x-1}\frac{\pi\eta}{(k_xL)^2}\sum_{l=0}^{\infty}\frac{\Gamma(3+2l)}{\Gamma(2+l)}\left(\xi\frac{\bar{k}_{yz}a}{2}\right)^l J_l(\bar{k}_{yz}a)\times\sum_{m=0}^{l}(-1)^m\frac{1}{\Gamma(2+2l-2m)}\left(\frac{2}{k_xL}\right)^{2m}, \tag{18}$$

where $\Gamma(n)$ is the complete gamma function.

The expressions of $F(\bar{k}_{yz},k_x)$ and $I(\bar{k}_{yz},k_x)$ for some special values of $\bar{k}_{yz}$ and k_x are as follows:

$$F(0,k_x)=\frac{4\pi\eta}{k_x^3L^3}\left[\sin(k_xa)-(k_xa)\cos(k_xa)+k_x\frac{L}{2}\cos\left(k_x\frac{L}{2}\right)\right], \tag{19}$$

$$I(0,k_x)=-2\pi\eta\frac{\cos(k_xL/2)}{(k_xL)^2}; \tag{20}$$

$$F(0,0)=\frac{2\pi\eta}{3L^3}h^2(3a-h), \tag{21}$$

$$I(0,0)=\pi\eta\left[\frac{a^2}{L^2}-\frac{1}{12}\right], \tag{22}$$

where $h=a-L/2$. By use of Eq. (21) or Eq. (22), we can give the expression of volume fraction of inclusions in this case as

$$p_1=\theta_1^{(\mathrm{oe})}(\mathbf{k}=0)=2I(0,0)-\theta_1^{(\mathrm{noe})}(\mathbf{k}=0)=\frac{4\pi\eta}{3}\left[\frac{3}{2}\left(\frac{a}{L}\right)^2-\left(\frac{a}{L}\right)^3-\frac{1}{8}\right]. \tag{23}$$

III. NUMERICAL RESULTS AND DISCUSSION

By imposing an electric field $\mathbf{E}_0$ along the direction of the minor axes of the oblate spheroids, i.e., the z direction, the frequency dependences of the modulus of enhancement factor in the direction of the minor axes of the oblate spheroids $|g_e^{zz}|$ of the MI and semiconductor-insulator (SI) composites with various kinds of geometric microstructure are calculated. First, the expansion coefficients $\mathbf{C}_l^E(\mathbf{r})$ are calculated by using Eq. (6). A truncated reciprocal lattice, n_x, n_y, and n_z of which varies from $-N$ to $+N$, is adopted. The numerical results indicate that $N=30$ is enough to ensure the convergency of these coefficients. Then $\mathbf{E}_{lin}(\mathbf{r})$ is calculated by use of the series expression in Eq. (4). The Padé approximant[16,17] is used in the calculations. Our calculations show that the Padé approximant can give good convergent results when the first 17 terms of the series are used. Adding more terms improves the convergency a little. Symmetry is imposed to reduce the area used in the calculations to one eighth of the unit-cell area. A mesh is generated. The electric field at the center of each division of the mesh is calculated. Finally, by substituting the values of $\mathbf{E}_{lin}(\mathbf{r})$ into Eq. (2), we can evaluate the nonlinear susceptibility for the composites.

A. Metal-insulator composite

For MI composites we adopt the Drude model for the dielectric function of the metal inclusions,

$$\varepsilon_1=1-\frac{\omega_p^2\tau}{\omega(\omega\tau+i)}, \tag{24}$$

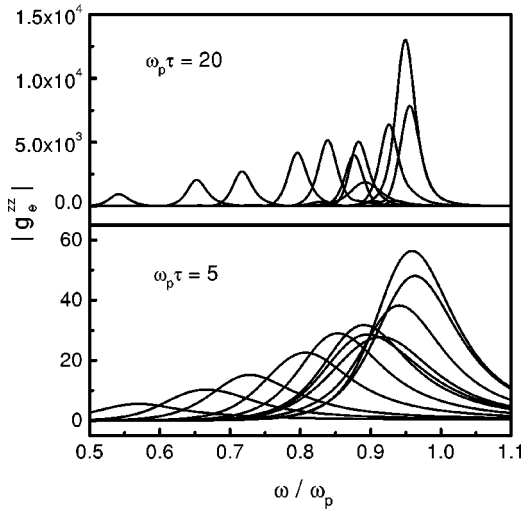

FIG. 2. $|g_e^{zz}|-\omega$ curves for a fixed volume fraction of metal phase $p_1=0.1$ and $\omega_p\tau=5,20$. For each fixed $\omega_p\tau$, η is 1.0, 0.6667, 0.5, 0.3333, 0.25, 0.2, 0.191 ($\eta_c^{(1)}$, the percolation threshold), 0.1818, 0.1429, 0.0879 ($\eta_c^{(2)}$), and 0 (perfect layered composite) from left to right.

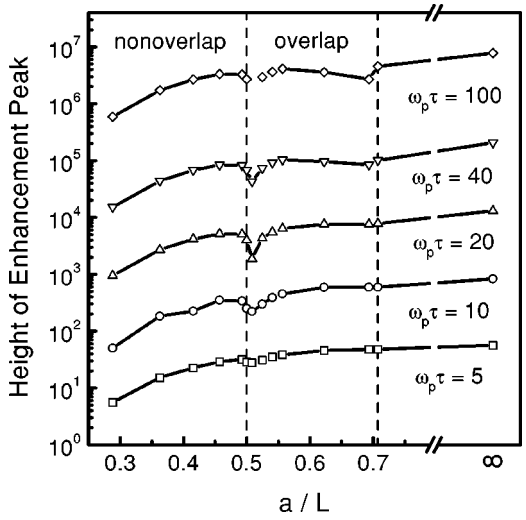

FIG. 3. HEP versus a/L for a fixed volume fraction of metal phase $p_1=0.1$ and $\omega_p\tau=5$, 10, 20, 40, and 100. The points of the right end of each curve are the results for perfect layered composites. The values of a/L at left vertical dashed line and at right one correspond to $\eta_c^{(1)}$ and $\eta_c^{(2)}$, respectively.

where ω_p denotes the plasmon frequency and τ is a characteristic relaxation time. We choose the frequency independent dielectric constant of the insulating host $\varepsilon_2=1$.

The modulus of enhancement factor $|g_e^{zz}|$ as a function of frequency ω for a fixed volume fraction $p_1=0.1$ and several values of $\omega_p\tau$ ranging from 5 to 100 is calculated. In the calculations, a series of values of η ranging from 1 to 0 is adopted, which represents various kinds of microstructure of the composites from the granular composites to the layered ones. In Fig. 2 we show the modulus of enhancement factor $|g_e^{zz}|$ as a function of frequency ω for $\omega_p\tau=5,20$, and several values of η. The results for $\eta=0$, that is, for the perfect layer structure, are obtained from the relation given by Boyd and Sipe.[13] It can be seen in this figure that there is a nonlinearity enhancement peak in each $|g_e^{zz}|-\omega$ curve. For each fixed value of η, the width of the enhancement peak lessens while the position of the enhancement peak (PEP) keeps almost unshift with an increase in $\omega_p\tau$. It can also be seen that the anisotropic morphology of the composites has pronounced effects on the nonlinearity enhancement. As the morphology of the inclusions is changed from spherical to oblate spheroid and further to layered network, that is, η lessens from 1 to 0, the nonlinearity enhancement is increased to orders of magnitude while the PEP obviously shifts to the high frequency.

In Fig. 3 we show the dependence of the height of the enhancement peaks (HEP) on the geometric anisotropy of inclusions for several values of $\omega_p\tau$. In this figure the geometric anisotropy of inclusions is represented by a length scale a/L instead of η. For a fixed volume fraction p_1, a/L is a function of η and can be obtained by use of Eq. (10) in the case of nonoverlapping inclusions and by use of Eq. (23) in the case of overlapping inclusions. It is shown in this figure that the HEP increases rapidly with an increase in $\omega_p\tau$. For each fixed value of $\omega_p\tau$, the HEP increases rapidly with the increase of geometric anisotropy of the inclusions for the granular composites. The HEP increases almost to its maximum as the composites are near the percolation threshold. A local minimum appears at the percolation threshold ($a/L\approx0.508$) in each HEP$-a/L$ curve. The depth of the local minima increases as $\omega_p\tau$ increases. The conclusion is similar to that proposed recently by Sarychev and Shalaev.[7] The HEP reaches its maximum as the composites with spheroidal-shaped inclusions are transformed into the composites with a perfect layer structure, that is, the Boyd-Sipe-type layered composites.

The dependences of the nonlinearity enhancement of the composites on the volume fraction of inclusions for geometric isotropy composites, i.e., the composites with spherical

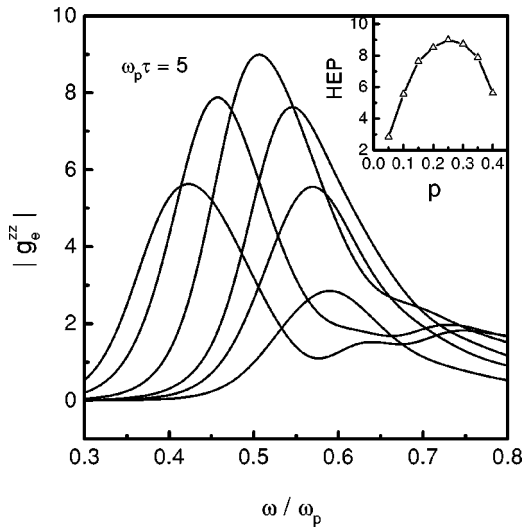

FIG. 4. $|g_e^{zz}|-\omega$ curves in the case of the spherical inclusions for several values of a volume fraction of metal phase p ranging in order of 0.4, 0.35, 0.25, 0.15, 0.1, and 0.05 from left to right. Here, $\omega_p\tau=5$. HEP versus p is illustrated in the inset.

inclusions, are also investigated. We plot $|g_e^{zz}|-\omega$ curves in Fig. 4 for several values of volume fraction p_1 ranging from 0.05 to 0.4. It can be seen that for this kind of geometric microstructure, when $p_1<0.25$ the nonlinearity enhancement increases with an increase in p_1 and reaches maximum at $p_1\approx 0.25$, then it decreases with further increase in p_1. This result coincide with the experimental ones for MI ($Au:SiO_2$) granular composite films measured by a degenerate four wave mixing scheme[12]. Comparing this figure with Fig. 2, we can see that the increase in the nonlinearity enhancement from the geometric anisotropy of the composites is far larger than that from the increase in the volume fraction of metal phase.

B. Semiconductor-insulator composite

For SI composites we adopt the Lorentz oscillator model for the dielectric function of the semiconductor inclusions,

$$\varepsilon_1=\varepsilon_\infty+\frac{\omega_0^2}{\omega_1^2-\omega^2-i\gamma\omega}, \tag{25}$$

with

$$\omega_0^2=Ne^2\varepsilon_\infty/\varepsilon_0 m_0, \tag{26}$$

where ω_1 is the bound-electron resonant frequency, γ is the damping coefficient, and N,e, and m_0 are the bound-electron number density, charge, and effective mass, respectively. The dielectric constant in vacuum is ε_0. We choose $\omega_0=1$, $\omega_1=0.5$, $\gamma=0.08$, $\varepsilon_\infty=9$. With these choices, ε_1 is a reasonable simplified approximation to the complex dielectric function of GaAs.[5] The nonlinear susceptibility of the semiconductor χ_1 is taken to be unitary in our calculations.

As has been done for the MI composites, the effects of the anisotropic morphology on the nonlinearity enhancement for the SI composites are also investigated. The modulus of enhancement factor $|g_e^{zz}|$ as a function of frequency ω is calculated for various values of physical parameters and various kinds of microstructures of the composites.

In the calculations we found that the nonlinear optical responses of the SI composites sensitively depend on the dielectric constant of the insulating host ε_2. There is no significant nonlinearity enhancement when the value of ε_2 is small, and the enhancement obviously increases with an increase in ε_2. This result is in analogy to that obtained with the formulas by Haus *et al.*[4] The results presented in the following are obtained for $\varepsilon_2=25$ which has been adopted in Ref. 5. The $|g_e^{zz}|-\omega$ curves are plotted in Fig. 5 for a series of values of η and several values of $\omega_0=1.0$, 1.75, and 2.5, respectively. The results are obtained for a fixed volume fraction of inclusions $p_1=0.1$ and the values of the other parameters are the same as those chosen above. The results for $\eta=0$ are also obtained from the Boyd-Sipe relation.[13] Similar to the results for the MI composites, there is a sharp nonlinearity enhancement peak in each $|g_e^{zz}|-\omega$ curve; the nonlinearity enhancement is increased to orders of magnitude with a decrease in η; and the HEP reaches its maximum as the composites with spheroidal-shaped inclusions are transformed into the composites with a perfect layer structure. For each fixed value of ω_0, the PEP keeps almost unshift as η varies. This result is different from that for MI composites.

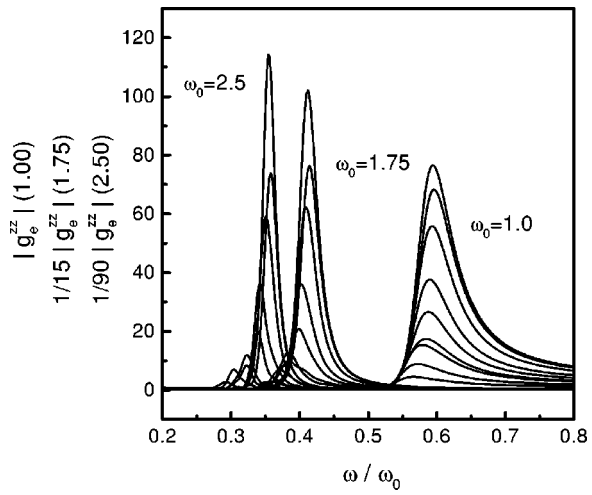

FIG. 5. $|g_e^{zz}|-\omega$ curves for a fixed volume fraction of semiconductor phase $p_1=0.1$ and $\omega_0=1.0$, 1.75, and 2.5. For each fixed $\omega_p\tau$, η is 1.0, 0.6667, 0.5, 0.3333, 0.25, 0.2, 0.191 ($\eta_c^{(1)}$, the percolation threshold), 0.1818, 0.1429, 0.0879 ($\eta_c^{(2)}$), and 0 (perfect layered composite) from bottom to top.

Calculations are carried out for different values of the physical parameters appearing in the expression for the dielectric function of the semiconductor phase. The results show that ω_0 has remarkable effect on the nonlinearity optical properties of the composites, especially for the composites near the percolation threshold. In Fig. 6 we show the dependences of the HEP on the geometric anisotropy of inclusions as a function of a/L for several values of $\omega_0=1.0$, 1.75, and 2.5, respectively. It can be seen that the HEP$-a/L$ curves have the features similar to those in the MI composites. Whereas there is no local minimum in HEP$-a/L$ curve in the case of $\omega_0=1.0$, a local minimum appears at the percolation threshold in each HEP$-a/L$ curve

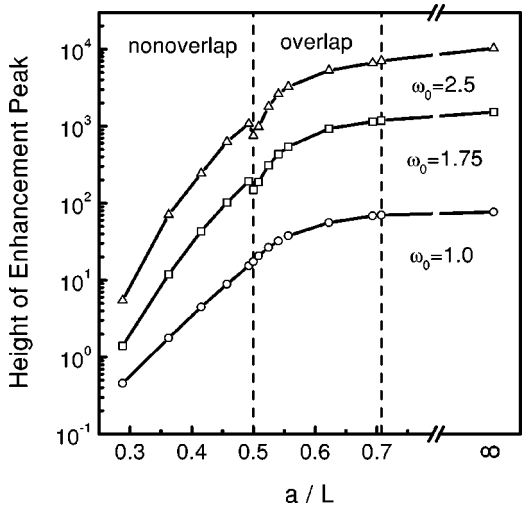

FIG. 6. HEP versus a/L for a fixed volume fraction of semiconductor phase $p_1=0.1$ and $\omega_0=1.0$, 1.75, and 2.5.

in two cases of $\omega_0=1.75$ and $\omega_0=2.5$. Because the results are obtained with the same value of ε_∞, we can see from Eq. (26) that different values of ω_0 corresponds to the different values of the ratio of the bound-electron number density to the effective mass of the electron, N/m_0. Therefore we conclude that the behavior of the nonlinear optical responses at the percolation threshold depends on N/m_0 in the SI composites with geometric anisotropy. When the value of the ratio N/m_0 is large, the minimum appears in the nonlinear optical responses at the percolation threshold.

IV. SUMMARY

Granular composites are usually disordered on the microscale. Recently, the researches on highly ordered periodic granular composites, such as photonic crystal and electrorheological fluid, have been very active. Periodic composites can be much more easily analyzed and some significative conclusions can be gained from the investigations on the effect of microstructure on the effective properties of the composites. In this paper, we have investigated the third-order optical nonlinearity enhancement for the MI and SI composites with periodic anisotropic microstructure. The composites are composed of metal or semiconductor spheroids embedded in an insulating host in a simple cubic lattice. The frequency dependences of the effective nonlinear susceptibility of the composites have been evaluated as a function of the geometric anisotropy of the inclusions and the effects of geometric anisotropy on the nonlinearity enhancement have been discussed. By tuning the shape of the inclusions from spherical particles to oblate spheroids, one can increase the nonlinearity enhancement of the composites by orders of magnitude. Meantime, the response frequency obviously shifts to high frequency for the MI composites and keeps almost unshift for the SI composites. These results are qualitatively similar to those in our previous reports,[18] in which we investigated the effect of geometric anisotropy on optical nonlinearity enhancement for the composites composed of infinitely long nonlinear metal or semiconductor cylinders with elliptic cross section parallelly embedded in an insulating host in a rectangular array.

The extreme case of anisotropic microstructure of the composites is a layered structure with flat interface. The results in this case are highly consistent with those calculated by use of the Boyd-Sipe relation for a layered composite. We compare the results of our calculation with those calculated by use of the Boyd-Sipe relation in layered composites, and we conclude that the nonlinearity enhancement increase to its maximum when the ordered granular composites are transformed into the Boyd-Sipe layered composites. This conclusion seems to be significant in designing and fabricating practical nonlinear-optical composite materials with a strongly nonlinear response.

The behavior of the nonlinearity enhancement of geometric anisotropy MI and SI composites near the percolation threshold has been studied. For the MI composites, the results show that there is a local minimum in each HEP $-a/L$ curve near the percolation threshold. The depth of the local minima increases with an increase in $\omega_p\tau$. The conclusion is similar to that proposed recently by Sarychev and Shalaev.[7] For the SI composites, the results show that the ratio of the bound-electron number density to the effective mass of the electron N/m_0 has remarkable effect on the nonlinearity optical properties of the composites near the percolation threshold, and a minimum appears in the nonlinear optical responses at the percolation threshold for large N/m_0.

ACKNOWLEDGMENTS

This work was supported by the National Science Foundation of China under Grant No. 59871033 and the Science Foundation of Hubei Province of China under Grant No. 2000J028.

[1] *Phase Conjugate Optics*, edited by J. J. Sakai (McGraw-Hill, Singapore, 1992).
[2] A. E. Neeves and M. H. Birnboim, J. Opt. Soc. Am. B **6**, 787 (1989).
[3] K. P. Yuen, M. F. Law, K. W. Yu, and Ping Sheng, Phys. Rev. E **56**, R1322 (1997); Opt. Commun. **148**, 197 (1998).
[4] J. W. Haus, R. Inguva, and C. M. Bowden, Phys. Rev. A **40**, 5729 (1989).
[5] D. Stroud and Van E. Wood, J. Opt. Soc. Am. B **6**, 778 (1989), and the references cited therein.
[6] B. F. Yang, C. X. Zhang, Y. S. Zheng, T. Q. Lu, X. H. Wu, W. H. Su, and S. Z. Wu, Phys. Rev. B **58**, 14 127 (1998).
[7] A. K. Sarychev and V. M. Shalaev, Phys. Rep. **335**, 275 (2000).
[8] D. Stroud and P. M. Hui, Phys. Rev. B **37**, 8719 (1988).
[9] X. Zhang and D. Stroud, Phys. Rev. B **49**, 944 (1994).
[10] V. M. Shalaev, Phys. Rep. **272**, 61 (1996).
[11] X. H. Wu, C. X. Zhang, and S. Z. Wu, Solid State Commun. **97**, 997 (1996); C. X. Zhang, X. H. Wu, S. Z. Wu, and W. H. Su, Phys. Rev. B **54**, 16 349 (1996).
[12] H. B. Liao, R. F. Xiao, J. S. Fu, P. Yu, G. K. L. Wong, and Ping Sheng, Appl. Phys. Lett. **70**, 1 (1997).
[13] R. W. Boyd and J. E. Sipe, J. Opt. Soc. Am. B **11**, 297 (1994).
[14] D. J. Bergman and K. J. Dunn, Phys. Rev. B **45**, 13 262 (1992); D. J. Bergman and D. Stroud, in *Solid State Physics*, edited by H. Ehrenreich and D. Turnbull (Academic, New York, 1992), Vol. 46, pp. 147–269.
[15] Yakov M. Strelniker and D. J. Bergman, Phys. Rev. B **50**, 14 001 (1994).
[16] G. A. Baker, Jr., *Essentials of Padé Approximants* (Academic, New York, 1975).
[17] G. A. Baker, Jr., and P. R. Graves-Morris, in *Encyclopedia of Mathematics and its Applications*, edited by G. C. Rota (Addison-Wesley, London, 1981), Vol. 13–14.
[18] B. F. Yang, C. X. Zhang, Q. Q. Wang, Z. H. Zhang, and D. C. Tian, Opt. Commun. **183**, 307 (2000); B. F. Yang, C. X. Zhang, Q. Q. Wang, and D. C. Tian, Appl. Phys. A: Mater. Sci. Process. **75**, 411 (2002).